Dynamic Behavior of Closed Grinding Systems and Effective PID Parameterization

TSAMATSOULIS DIMITRIS
Halyps Building Materials S.A., Italcementi Group
17th Klm Nat. Rd. Athens – Korinth
GREECE
d.tsamatsoulis@halyps.gr http://www.halyps.gr

Abstract: - The object of the present study is to investigate the dynamic of closed circuit cement mills and based on that to tune robust PID controllers applied to three actual installations. The model that has been developed, consisting of integral part, time delay and a first order filter, is based exclusively on industrial data sets collected in a period more than one year. The model parameters uncertainty is also assessed varying from 28% to 36% as the gain is concerning and 34% to 42% as regards the time delay. As significant sources of model uncertainty are determined the grinding of various cement types in the same cement mill and the decrease of the ball charge during the time. The Internal Model Control (IMC) and M - Constrained Integral Gain Optimization (MIGO) methods are utilized to adjust the controller parameters. Specially by implementing the MIGO technique robust controllers are built deriving a daily average IAE 2.3-3% of the set point value. Due to the high flexibility and effectiveness of MIGO, the controllers can be parameterized by taking into account the cement type ground and the power absorbed. Subsequently the attenuation of main uncertainties leads to improvement of the regulation performance.

Key-Words: - Dynamic**,** Cement, Mill, Grinding, Model, Uncertainty, PID, tuning, robustness, sensitivity

1 Introduction

Among the cement production processes, grinding is very critical as far as the energy consumption is concerned. On the other hand the grinding is very essential as to the product quality characteristics because during this process the cement acquires a certain composition and fineness. Because of these two reasons, grinding mostly is performed in closed circuits, where the product of the cement mill (CM) outlet is fed via a recycle elevator to a dynamic separator. The high fineness stream of the separator constitutes the final circuit product, while the coarse material returns back to CM to be ground again.

A simplified flow sheet, showing the basic components of a closed grinding system is demonstrated in the Figure 1.

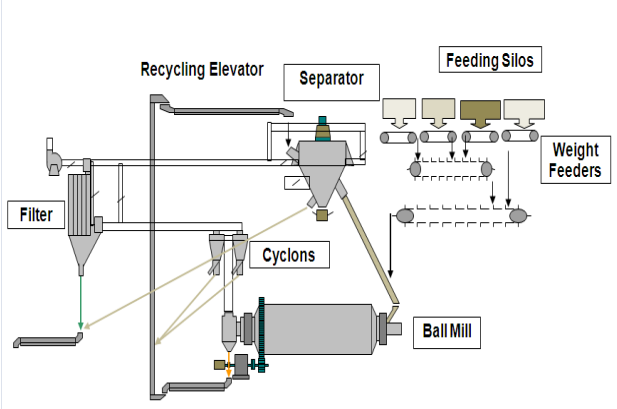

Figure 1.Closed circuit grinding system.

A contemporary cement production plant applies a continuous and often automatic control of the production as well as of the quality. These two operations should always be controlled and regulated simultaneously and in combination and never as individual ones. The automatic operation presents several advantages in comparison to the manual one [1, 2]. In the usual automatics one of the following has typically selected as process variable. (1) The power of the recycle elevator. (2) The return flow rate from the separator. (3) An electronic ear in the mill inlet. (4) The mill power or combination of the above.

Several studies describe numerous techniques of mills automation with varying degrees of complexity. Ramasamy et al. [3], Chen et al. [4] developed Model Predictive Control schemes for a ball mill grinding circuit. Because of the multivariable character, the high interaction between process variables and non – linearity always present in closed grinding systems, control schemes of this kind were developed [5, 6, 7, 8]. A survey of the industrial model predictive control technology has been provided by Qin et al. [9]. The common between all these efforts and designs is the assumption of a model describing the process dynamics. However it has been mentioned by Astrom et al. [10] that in the industrial process

control more than 95% of the control loops are of PID type and moreover only a small portion of them operate properly as Ender [11] points out. Frequently also the controller parameters are tuned with trial and error [12], because of the lack of a model or of high model uncertainty. To overcome such difficulties fuzzy PID controllers have been also recently developed [13] and the pseudo-equivalence with the linear PID was proven. As it was clearly stated by Astrom [14], model uncertainty and robustness have been a central theme in the development of the field of automatic control. Subsequently it is of high importance not only to describe a process using a representative model, but to estimate the parameters uncertainty as well. This consideration can facilitate the design of a robust controller.

Two models of the dynamic behavior of closed circuit grinding systems are developed and a detailed analysis of the model parameters uncertainty is attempted. Actual industrial data of three cement mills – CM5, CM6 and CM7 - of the Halyps Cement Plant are considered collected in a long term period, where various cement types were ground. The above analysis could lead to the design and parameterization of a robust controller of PID type, which is usually the industrial case.

In spite of all the advances of the control during the last decades the PID controller remains the most common one. Because of their simplicity of implementation, these controllers are extensively used in industrial applications [15]. In spite the numerous papers written on tuning of PID controllers, it remains a challenge to adjust effectively, existing and operating PID loops, installed in grinding systems as the mentioned ones, where a detailed analysis of the dynamic behavior has been performed.

Nyquist-like design methods are proposed to handle uncertainties in a straightforward way, as the classical Z-N tuning (Ziegler and Nichols) [16] and BLT method [17].

A widely applied technique to tune PID controllers is this of Internal Model Control (IMC). Garcia, Morari and Rivera developed Internal Model Control [18, 19, 20, 21]. Morari and Zafiriou [22] summarized Internal Model Control over a wide range of control problems. Yamada presented a modified IMC for unstable systems [23]. Essential also contribution had Cooper [24] and Skogestad [25, 26] to the IMC implementation.

Another extensively applied tuning methodology is the robust loop shaping [27, 28, 29, 30, 31]. A very effective loop shaping technique to tune PID controllers was proven to be the called MIGO (M-constrained integral gain optimization) [32, 33, 34, 35]. The design approach was to maximize integral gain subject to a constraint on the maximum sensitivity. There are also other successful attempts to design PID controllers in the frequency domain and to characterize their performance [36, 37].

The investigation gives interesting insights and tries to provide answer to the following question: When is it worthwhile to do more accurate modeling, to search for enduring sources of uncertainty and to reject them permanently if possible? Two tuning methodologies are applied and the resulting controllers are utilized to regulate three CM operations under highly uncertain conditions

2 Model Development

In all the cases the response of the recycle elevator power to mill fresh feed disturbances is examined. According to Astrom et al. [38], there is a limited order of models, which can be applied to linear and time invariant systems or systems approaching this state. Primarily the system stability under the given operating conditions has to be analyzed, e.g. if a step change of the fresh feed, leads to a new steady state of the elevator power. In the opposite case the system transfer function contains integral part. The delay time between a disturbance of the fresh feed and the elevator response shall be investigated. To estimate the above the doublet pulse method is applied [10]. A typical example of the application of the method is demonstrated in the Figure 2, concerning CM5. The difference of KW from the initial value is plotted as function of the difference of the mass flow rate from its initial one.

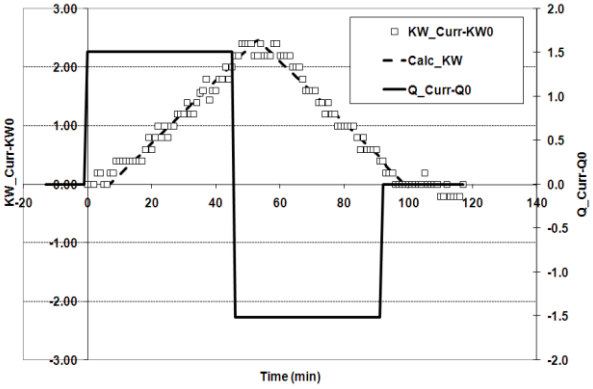

Figure 2.Example of doublet pulse method.

From the Figure 2 it is concluded that in the specified operating region of the elevator power the process involves integration. Additionally, to avoid undesirable noise, a first order filter is added to the power signal with time constant T_f equal to 3 min. Two models are selected to describe the system

dynamics: The first does not take into account the first order filter and includes only the integrating action and the time delay. To compensate the filtering action and the different system behavior when the recycle elevator power is increasing or decreasing, two transfer functions are designed represented in Laplace form by the equations (1), (2).

$$KW - KW_0 = (Q - Q_0)\frac{k_{v1}}{s}e^{-Td\cdot s} \quad (1)$$

$$KW - KW_0 = (Q - Q_0)\frac{k_{v2}}{s}e^{-Td\cdot s} \quad (2)$$

where Q = the mass flow rate (tn/h), KW = $P/P_{Max}\cdot 100$, the percentage of the power P of the recycle elevator to the maximum installed power P_{Max}, Q_0 = the flow rate corresponding to power percentage KW_0 of the steady state, k_{v1}, k_{v2}= the gains (h/tn) when the elevator is increasing and decreasing correspondingly and T_d= the delay time (min),.

The second model incorporates the first order filter actually existing. Consequently the model is described by the following equation:

$$KW - KW_0 = (Q - Q_0)\frac{k_v}{s\cdot(1+T_f s)}e^{-Td\cdot s} \quad (3)$$

The meaning of the model parameters and variables is exactly the same as in the first one. Apparently the two models constitute a simplification of the actual process. If they describe adequately the CM dynamic behavior shall be verified from the comparison between the actual and calculated values. It must be taken into account that for the parameterization of a controller, the simplest possible model shall be chosen. Then, the quality of the regulation is a function of the model accuracy [39]. It shall also be clarified that mathematical models have been developed, describing with extraordinary adequacy the grinding process [40, 41, 42]. However frequently, due to their complicated structure, the corresponding transfer function is extremely difficult or impossible to be derived.

By substituting the flow rate term of the above equations with the input signal u, and the power term with the output signal e, equations (1), (2), take the form of the equations (4), (5) respectively, while equation (3) is transformed to the formula (6) representing the transfer function of the process G_p for the two models under consideration:

$$\frac{e}{u} = \frac{k_{v1}}{s}e^{-Td\cdot s} \quad (4)$$

$$\frac{e}{u} = \frac{k_{v2}}{s}e^{-Td\cdot s} \quad (5)$$

$$\frac{e}{u} = \frac{k_v}{s\cdot(1+T_f s)}e^{-Td\cdot s} \quad (6)$$

The set of the model parameters includes the gain k_v, the delay time T_d, as well as the flow rate Q_0 and power KW_0, corresponding to the system steady state, under the specified any time operating conditions of the grinding circuit concerning (a) cement type, (b) raw materials moisture and grindability, (c) gas flows, (d) pressures, (e) temperatures, (f) condition of the grinding media, (g) separator efficiency etc. The variety of these conditions generates the model uncertainty as concerns the parameters values. Therefore the first model includes six independent parameters while the second one only four, but its form is relatively more complicated that the first one. The first model has the advantage that simpler PID tuning techniques can be applied, while the second describes more accurately the process.

The model parameters are calculated by applying the convolution theorem between the input signal u and the process variable e, expressed by the equation (7).

$$e = \int_0^t u(\tau)\cdot g(t-\tau)d\tau \quad (7)$$

Where g(t) is the pulse system response. Exclusively industrial data of routine operation of the CM are utilized. These data are sampled on-line by using convenient software. Time intervals equal to 250 minutes of continuous mill operation are selected as individual sets of data and the parameters are estimated for each separate set, by using a non-linear regression technique. For this purpose software in Visual Basic for Applications was developed. As a result, the experimental estimation of the parameters by applying the doublet pulse method is avoided as it presents some severe disadvantages: (a) The feed disturbance results in a disturbance in the production process, having in parallel an impact on the product quality. (b) As the process contains integration, the achievement of a steady state condition, required by the method, is not easy at all. (c) To have an estimation of the range the dynamic parameters are

varying, a large number of experiments are needed to have a reliable approximation of their uncertainty.

3 Results of the Dynamical Models and Discussion

3.1 Models Adequacy

Due to the large variety of uncertainty sources, a sizeable number of experimental sets are normally required to assess if the models are adequate to describe the process and to investigate as well the parameters uncertainty. The number of industrial sets for each model follows in the Tables 1 and 2, comprising the corresponding number of months to get these results. The experimental set where the first model was applied is a subset of the corresponding set of the second model. The reason is that using the first model, the initial tuning of the controllers was implemented by following the Internal Model Control (IMC) technique. As data were accumulated and using a bigger set the loop shaping technique was implemented and the controllers were tuned.

Table 1. Experimental sets of the first model

	Number of Sets	Months
CM5	289	3
CM7	174	2

Table 2. Experimental sets of the second model

	Number of Sets	Months
CM5	1598	17
CM6	427	7
CM7	604	15

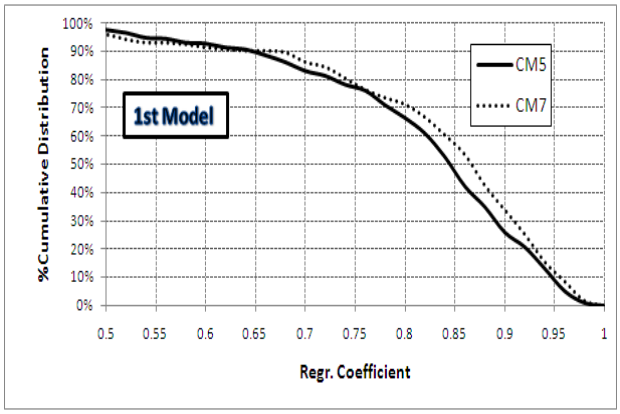

Figure 3. Cumulative distribution of the regression coefficients of the first model.

To check the model adequacy, the cumulative distribution of the regression coefficients is estimated. The results for the three cement mills are presented in the Figures 3 and 4 for the two models. As it can be concluded from these figures, the models describe adequately the process, as 75% to 85% of the regression coefficients are higher than 0.7. Consequently both models fit with good accuracy the experimental data and they can be utilized for tuning of the existing PID controllers.

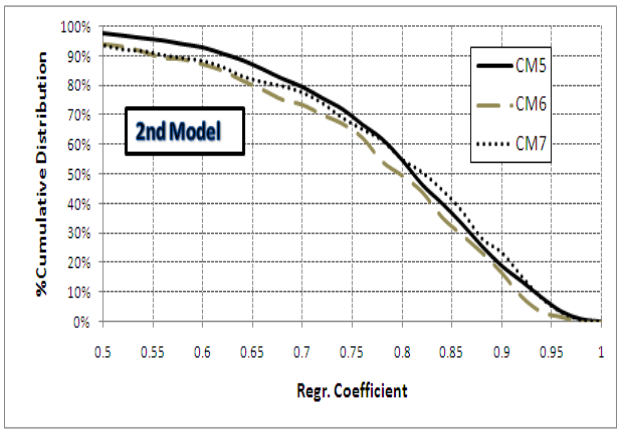

Figure 4. Cumulative distribution of the regression coefficients of the second model.

The residual errors of each model applied to each mill are given by the equation (8) and follow the χ^2 distribution:

$$s_{res}^2 = \sum_{I=1}^{N} \frac{(KW_{calc} - KW_{exp})^2}{N-k} \quad (8)$$

Where s_{res} = the residual error, KW_{calc} = the calculated from the model power of the recycle elevator, KW_{exp} = the actual one, N = the number of experimental points and k=the number of the independent model parameters. As it is known the χ^2 distribution is defined as following: If the independent random variables X_1, X_2, .. X_N follow the normal distribution with mean value and variance equal to 0 and 1 respectively, then the variable $\chi^2=\sum X_I^2$ follow the χ^2 distribution where as N the distribution degrees of freedom are defined. Normally the causes of model uncertainty including the model imperfection can be considered as independent normal variables and their overall action within a set of experimental data results in the corresponding residual error. Consequently using the experimental distribution of the residual variance the number of the freedom degrees of the χ^2 distribution can be calculated. This result can be considered as an estimation of the number of the permanent sources, causing the model uncertainty.

To calculate the above, the following procedure is applied:

- The cumulative distribution of the experimental s_{res}^2 is found with a step of 0.01 and an array of sorted variances s_I^2 is derived.
- The median value is calculated from this experimental distribution. This value is to be used as initial value for the calculation of the distribution mean,μ
- An initial value of degrees of freedom, df, is supposed.
- For each experimental cumulative probability P_I, corresponding to an experimental variance s_I^2 the calculated variance $s_{C,I}^2$ is computed by the formula (9):

$$s_{C,I}^2 = \frac{df-1}{\chi^2(P_I,df)} \cdot \mu \quad (9)$$

- The square error between s_I^2 and $s_{C,I}^2$ for all the I is determined and using non linear regression techniques the optimum degrees of freedom, df, and average value, μ, minimizing the above error are found.

The results for the different cement mills where the two models are applied are shown in the Table 3.

Table 3. χ^2 parameters of the residual variances

	Degrees of Freedom, df	Average Value, μ
First Model		
CM5	4	0.0757
CM7	4	0.1747
Second Model		
CM5	4	0.0816
CM6	3	0.1996
CM7	4	0.1747

From the table 3 it is concluded that the degrees of freedom and the attributed permanent sources of uncertainty are 3 – 4, e.g. for a given experimental set they are relatively low. Some of the mentioned ones (a) to (g) in the end of the section 2 can be considered as such sources. Therefore, as the control to these parameters is increasing and they are kept as constant as possible, less is the uncertainty and higher the ability to achieve a stable CM operation. On the other hand the tuning of a robust controller becomes more powerful. The experimental and calculated variances are demonstrated in the Figures 5 and 6. As it can be observed from these figures the fitting between experimental and calculated variances is very good.

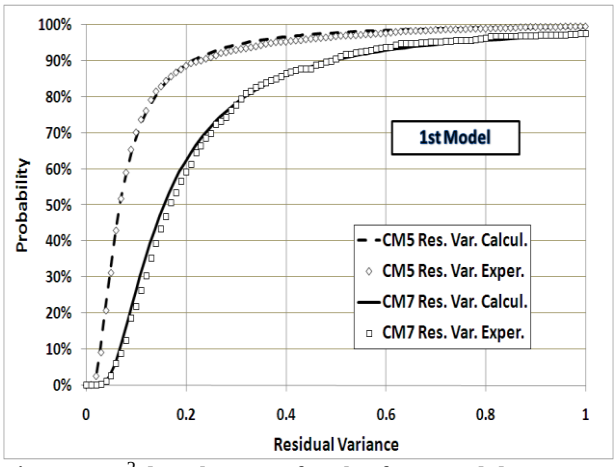

Figure 5. χ^2 distributions for the first model.

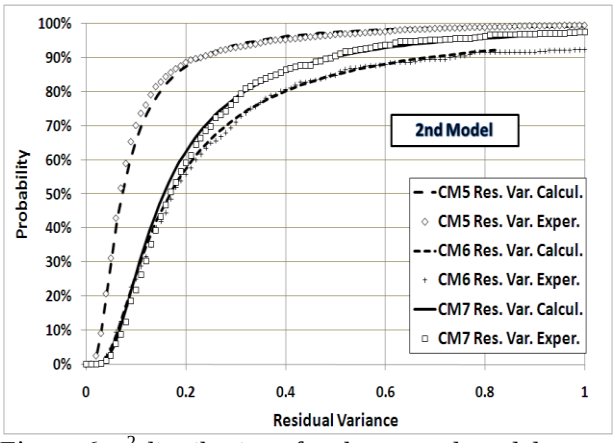

Figure 6. χ^2 distributions for the second model.

3.2 Function between Model Parameters and Regression Coefficient

The model parameters as average values as well as standard deviations are plotted against the regression coefficients, R, to check if there is any function between them. To implement the above, minimum R values are selected, R_Min, and the average and standard deviation of the model parameters for all the sets presenting R ≥ R_Min are calculated.

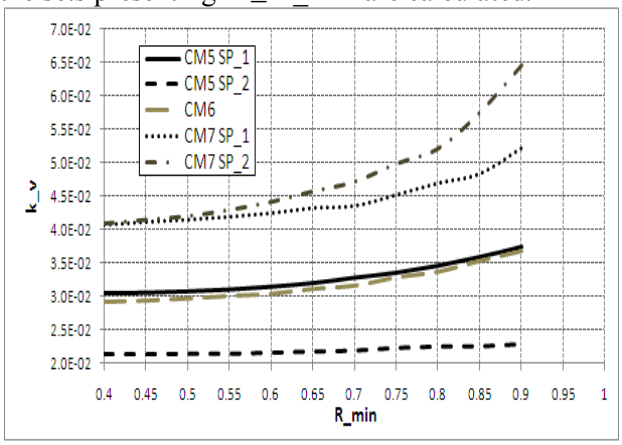

Figure 7. Function between average gain and R_Min

The results of these statistics of the gain k_v as function of R_Min are depicted in the figures 7 and 8 respectively. The second model parameters are chosen because of the larger number of experimental sets. During the period investigated, CM5 initially operated with a set point of the elevator power equal to 18% – SP 1 – and then with a set point equal to 26.7% - SP 2 - of the of the maximum power. The set point of CM7 was initially equal to 28% - SP 1 - and then 30% - SP 2 - of the maximum power. CM6 set point was always the same and equal to 36.6% of the maximum.

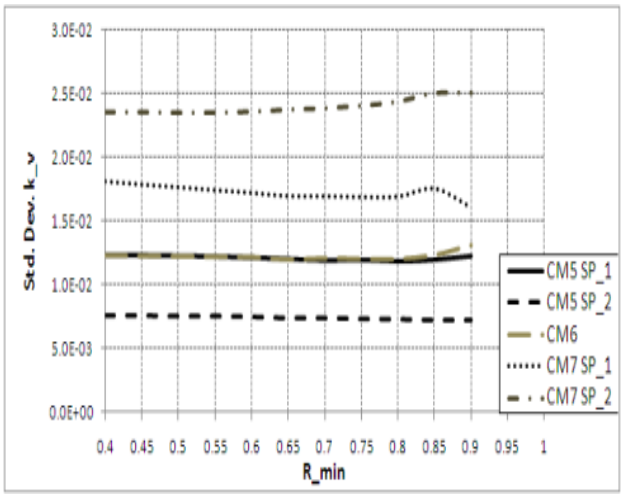

Figure 8. Function between standard deviation of gain and R_Min

A trend between the average gain and the R_Min can be observed from the Figure 7. As the model regression coefficient increases, the gain increases as well. That means that the disturbances not only affect the model accuracy, but also cause the estimation of a lower gain. Conversely the standard deviation of the gain is independent of the level of R_Min. As a result for all the range of R_Min, the model uncertainty remains practically invariant as the gain is concerning. This trend between R_Min and gain could be explained from the natural meaning of the gain: When a departure from the equilibrium point, $Q\text{-}Q_0$, occurs, then after T_d minutes, this change is transferred to the recycle elevator as $k_v \cdot (Q\text{-}Q_0)$, passing firstly from a first order filter with a time constant T_f. A model of poor accuracy is insufficient to predict the actual variation of the elevator power resulting in a calculated power change lower than the actual one, e.g. gain smaller than the actual.

An inverse impact appears in the case of delay time T_d as it can be observed from the Figures 9 and 10. The average delay time is independent from the level of the R_Min, while the standard deviation of the T_d, e.g. the delay time uncertainty shows a week trend to decrease as the R_Min increases.

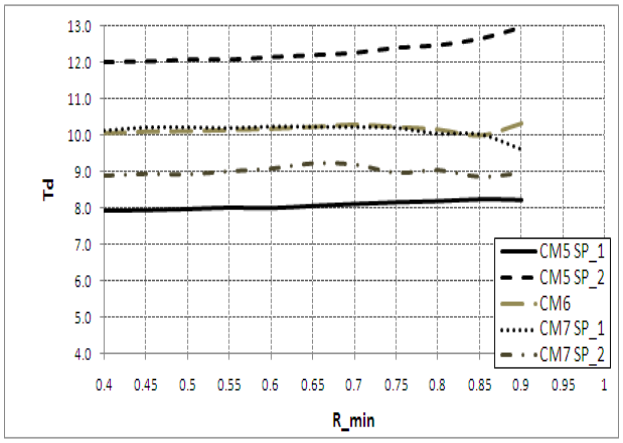

Figure 9. Average delay time as function of R_Min

Because of the trends presented in the Figures 7 to 10, to assure a lower level of parameters uncertainty, a relatively high value of regression coefficient R_Min has to be selected to assess the average model parameters and their uncertainty. As such value, R_Min=0.7 is chosen comprising the 75-85% of the total experimental sets.

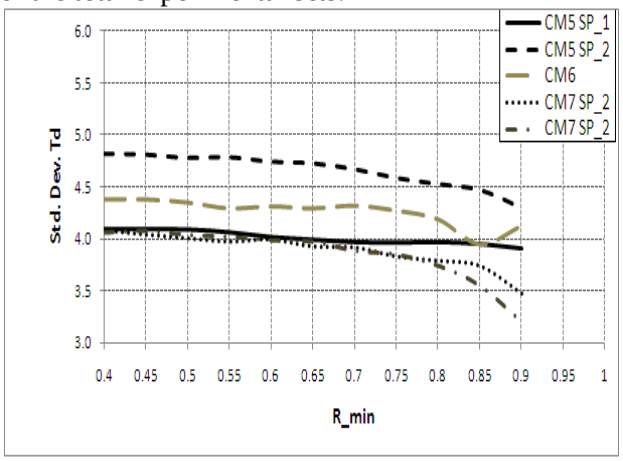

Figure 10. Standard deviation of T_d as function of R_Min

3.3 Evaluation of the Model Parameters and their Uncertainty

By filtering the model results, permitting to pass for further evaluations the sets representing a regression coefficient equal or higher than 0.7, the model parameters are determined as concerns their average value and standard deviation. To assess in a more precise way the model parameters uncertainty, by rejecting some values corresponding to low frequency disturbances, the "natural" deviation, σ_{NAT}, of the parameters is evaluated. To implement the above, the norm ISO 8258:1991 describing the

Sewhard control charts is utilized. To calculate this statistic the following steps are needed:
(a) Calculate the absolute range R_i between two consecutive parameters X_i, X_{i-1} and the average range R_{Aver}, over all the ranges population, by applying the equations (10):

$$R_i = |X_i - X_{i-1}| \qquad R_{Aver} = \frac{\sum_{i=1}^{N} R_i}{N} \tag{10}$$

(b) Calculate the maximum range, R_{Max}, for 99% probability provided by the formula (11). Each $R > R_{Max}$ is considered as an outlier and the values are excluded from further calculations.

$$R_{Max} = 3.267 \cdot R_{Aver} \tag{11}$$

(c) After the exclusion of all the outliers and calculation of a final R_{Aver}, the process natural deviation concerning the parameter under investigation is calculated using the equation (12):

$$\sigma_{NAT} = 0.8865 \cdot R_{Aver} \tag{12}$$

Table 4. First model parameters

	Cement Mills	
Parameters	CM5	CM7
Average k_{v1}	$3.0 \cdot 10^{-2}$	$4.8 \cdot 10^{-2}$
Std. Dev. k_{v1}	$1.6 \cdot 10^{-2}$	$2.7 \cdot 10^{-2}$
σ_{NAT} k_{v1}	$1.5 \cdot 10^{-2}$	$2.4 \cdot 10^{-2}$
%CV	49.8	55.8
Average k_{v2}	$3.2 \cdot 10^{-2}$	$4.1 \cdot 10^{-2}$
Std. Dev. k_{v2}	$1.6 \cdot 10^{-2}$	$2.7 \cdot 10^{-2}$
σ_{NAT} k_{v2}	$1.6 \cdot 10^{-2}$	$2.1 \cdot 10^{-2}$
%CV	50.0	51.7
Average T_d	10.2	13.9
Std. Dev. T_d	3.2	3.8
σ_{NAT} T_d	3.1	3.4
%CV	30.7	24.2
Average Q_0	25.8	33.4
Std. Dev. Q_0	0.9	1.4
%CV	3.5	4.1
Average KW_0	17.6	24.7
Std. Dev.KW_0	3.4	7.3
%CV	19.1	29.4
R_C_{Aver}	0.86	0.87

The parameters results concerning average values, standard and natural deviations for all the cement mills are presented in the Tables 4, 5, 6. The coefficients of variation of parameters, %CV and the average regression coefficients, R_C_{Aver} are also demonstrated.

Table 5. Second model parameters

	Cement Mills		
Parameters	CM5 SP 1	CM6	CM7 SP 1
Average k_v	$3.3 \cdot 10^{-2}$	$3.2 \cdot 10^{-2}$	$4.4 \cdot 10^{-2}$
Std. Dev. k_v	$1.2 \cdot 10^{-2}$	$1.2 \cdot 10^{-2}$	$1.7 \cdot 10^{-2}$
σ_{NAT} k_v	$9.1 \cdot 10^{-3}$	$1.1 \cdot 10^{-2}$	$1.6 \cdot 10^{-2}$
%CV	27.6	35.7	36.1
Average T_d	8.1	10.3	10.2
Std. Dev. T_d	4.0	4.3	3.9
σ_{NAT} T_d	3.4	4.0	3.5
%CV	41.6	39.0	34.4
Average Q_0	25.6	66.8	33.4
Std. Dev. Q_0	1.8	2.1	1.2
%CV	7.2	3.2	3.7
Average KW_0	17.6	36.6	26.4
Std. Dev.KW_0	3.4	6.6	6.3
%CV	19.3	18.0	23.7
R_C_{Aver}	0.86	0.84	0.86

Table 6. Second model parameters

	Cement Mills	
Parameters	CM5 SP 2	CM7 SP 2
Average k_v	$2.2 \cdot 10^{-2}$	$4.7 \cdot 10^{-2}$
Std. Dev. k_v	$7.7 \cdot 10^{-3}$	$2.4 \cdot 10^{-2}$
σ_{NAT} k_v	$6.3 \cdot 10^{-3}$	$1.6 \cdot 10^{-2}$
%CV	28.7	33.4
Average T_d	12.0	9.2
Std. Dev. T_d	4.6	3.9
σ_{NAT} T_d	4.1	3.5
%CV	34.1	38.2
Average Q_0	28.3	32.2
Std. Dev. Q_0	2.1	1.8
%CV	7.3	5.6
Average KW_0	26.4	30.8
Std. Dev.KW_0	3.8	7.8
%CV	14.4	25.4
R_C_{Aver}	0.89	0.84

In spite that the coefficients of variation are calculated using the natural deviation as the gain and delay time is concerning, they are very high for both models: For the first model 50-55% as to k_v and 24-31% as to T_d. The coefficients of variation, %CV, computed for the second model are 28-36% and 34-42 % as to k_v and T_d respectively. Especially for the second model, the cumulative distributions of the gain k_v and delay time T_d, for the three mills under consideration, are depicted in the Figures 11 and 12 respectively.

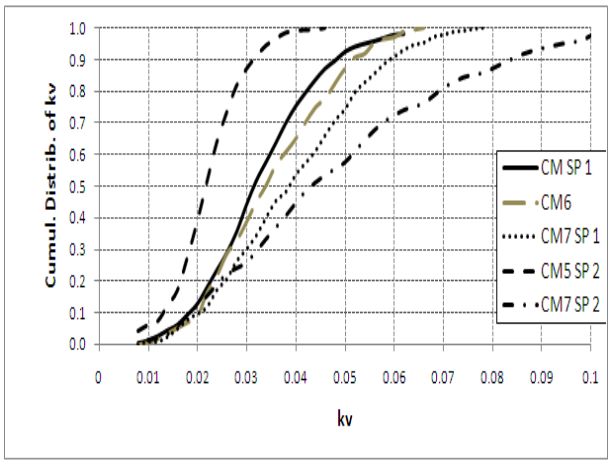

Figure 11. Cumulative distribution of k_v

From these two figures the high uncertainty of the model parameters becomes more obvious.

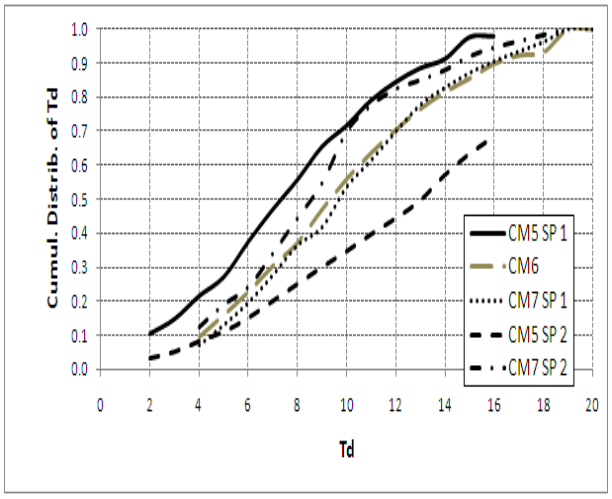

Figure 12. Cumulative distribution of T_d

To investigate if the normal distribution is good approximation of the gain and delay time distributions, the statistical norm ISO 2854-1976 is applied: For each cumulative experimental probability P_a, the corresponding normalized distance from the average, μ, in standard deviation σ, units, given by the formula (13) is computed.

$$z_a = \frac{z-\mu}{\sigma} \tag{13}$$

The gain and the delay time are plotted against the variable z_a. The better a straight line fits the resulting points, the higher the approximation by a normal distribution is. The mean value of the distribution corresponds to z_a=0, while the distribution standard deviation is equal to the slope. The k_v and T_d curves related to each mill and set point are depicted in the Figures 13 to 16.

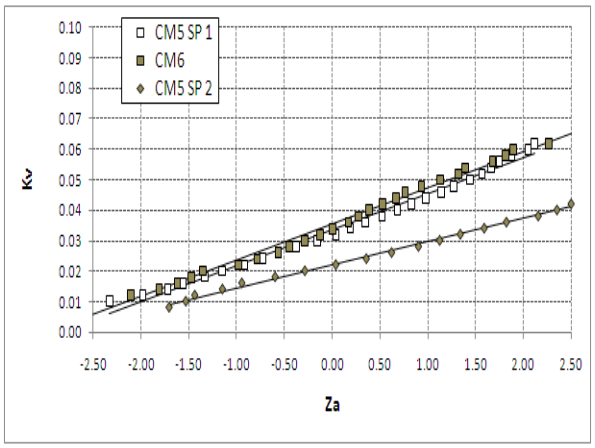

Figure 13. k_v as a function of the variable z_a – CM5, CM6

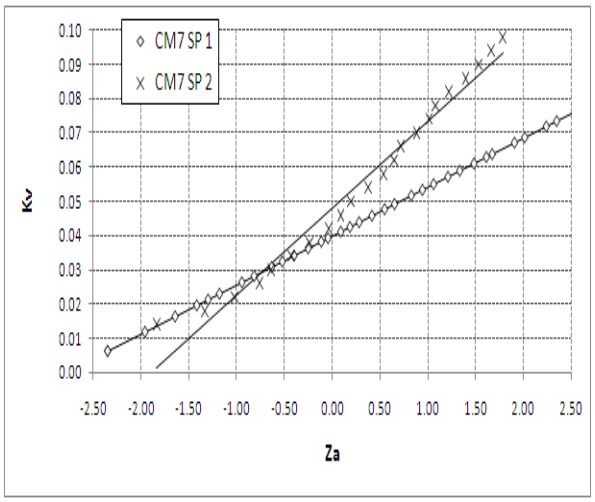

Figure 14. k_v as a function of the variable z_a – CM7

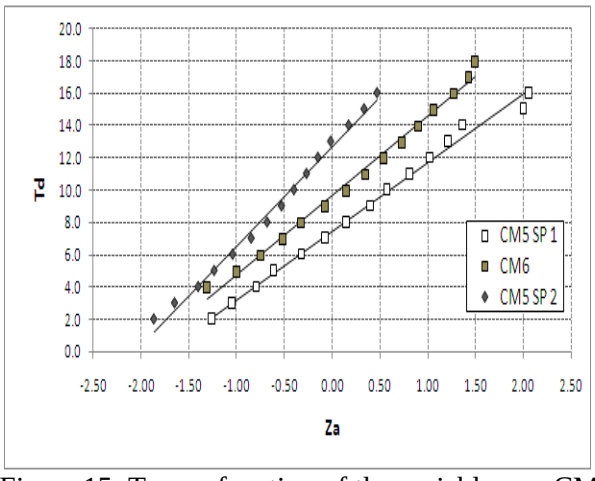

Figure 15. T_d as a function of the variable z_a – CM5, CM6

From the Figures 13 to 16 it is concluded that the dynamic parameters follow in the most cases the normal distribution with a good approximation. Probably only the gain for CM7 and set point 2

show a relatively significant departure from the normality.

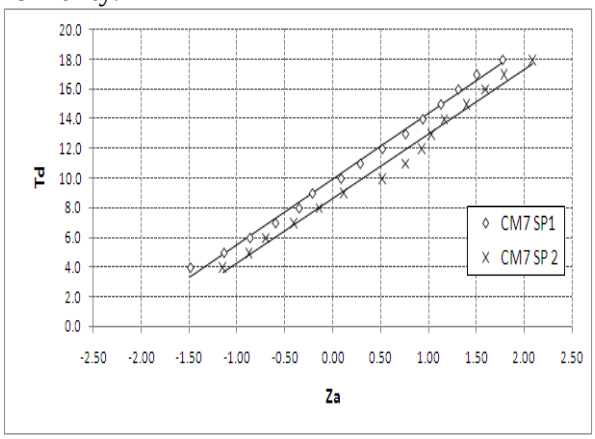

Figure 16. T_d as a function of the variable z_a – CM7

Some also important conclusions can also be extracted as concerns the impact of the set point value on the parameters uncertainty:

- The significantly larger SP 2 than SP 1 in the case of CM5 leads to a lower gain and a higher delay time. For a higher set point, the elevator is more loaded with material, so the same increase of the feed and of the variable $Q-Q_0$, results in a lower increase of the $(KW-KW_0)/(Q-Q_0)$ variable. For the same reason any change of the feed, will appear later to the recycle elevator, resulting in an increase of the delay time. The Niquist plots of the CM5 transfer functions for the two set points and demonstrated in the Figure 17. The X-axis and Y-axis represent the transfer function real and imaginary part respectively for different frequencies ω.
- Because the difference between SP 1 and SP 2 in CM7 is small, the delay times are similar. Other reasons shall be searched to find the important difference in the gains.

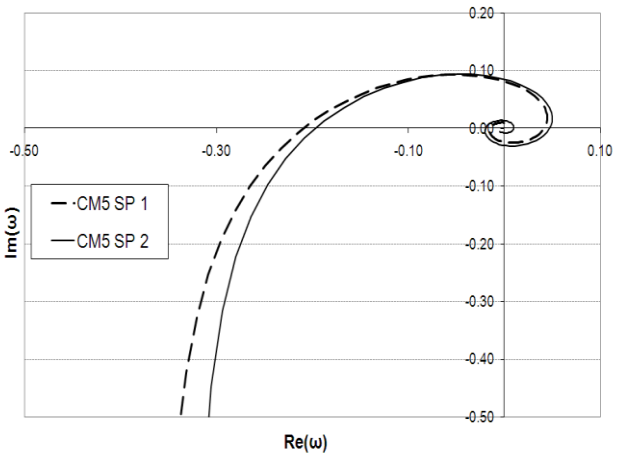

Figure 17. Niquist plots of the CM5 transfer functions for the 2 set points

The probable covariance between the model parameters is also investigated. As indicator of such covariance, the regression coefficient, R, between two populations of parameters is considered. Each parameter pair corresponds to the same experimental set. For each cement mill and set point a table of regression coefficients is calculated and the average R over the three CM is then found. The results are shown in the table 7.

Table 7. Parameters regression coefficients

	T_d	k_v	Q_0	KW_0
T_d	1	-0.093	0.011	-0.008
k_v		1	-0.077	0.039
Q_0			1	0.184
KW_0				1

From the Table 7, a positive week correlation can be observed between Q_0 and KW_0: In the case the feed is stabilized in a feed rate Q_0, then as Q_0 increases, KW_0 also enlarges. The power augmentation of the recycle elevator is the result of the rise of the circuit circulating load as the feed flow rate increases. A negative also week correlation seems to exist between T_d and k_v caused probably from material accumulation inside the CM.

3.4 Impact of the Cement Composition on the Parameters Uncertainty

Except the CM7 where one cement type is ground primarily, the two other cement mills process mainly three types. In the following analysis the subsequent codification is used as concerns the cement types: 1=CEM II A-L 42.5, 2=CEM IV B (P-W) 32.5, 3=CEM II B-M (P-L) 32.5. The composition of these cements according to EN 197-1 is given in the table 8 as to the main components. As it can be observed from this table the three cement types differ significantly in the clinker content and the other main components as well. Subsequently, there is a big probability the grinding of each one to show different dynamic, resulting in a source of uncertainty of the model parameters.

Table 8. Cement compositions

Cement	Clinker	Lime-stone	Pozzo-lane	Fly ash
1	80-94	16-20	-	-
2	45-64	-	36-55	
3	65-79	21-35		-

For the cement mills 5 and 6 and for each cement type, the second model parameters and their

standard deviation are calculated. The percentage of time that each mill grinds each type is also evaluated and illustrated in the Table 9.

Table 9. Percentage of time of each CEM type

CEM Type	CM5 SP 1	CM5 SP 2	CM6	CM7 SP 1	CM7 SP 2
1	8	7	34.6	100	66.4
2	61.9	37.8	18.5		
3	30.1	55.2	46.9		33.6

From the table 9 it is concluded that CM5 grinds primarily CEM IV B (P-W) and CEM II B-M (P-L) but also some significant quantities of CEM II A-L. On the contrary CM6 grinds mainly CEM II A-L and CEM II B-M (P-L) and not negligible quantities of CEM IV B (P-W) too. The gains and time delay results for all cases investigated are presented in the Table 10. These values are compared with the ones shown in the Tables 5, 6.

Table 10. Average values of the parameters

Type	CM5 SP 1		CM6	
	Average	Std.Dev	Average	Std.Dev.
	$k_v \times 10^2$			
All	3.3	1.2	3.2	1.2
1	3.5	1.5	3.0	1.1
2	3.0	1.0	3.0	1.2
3	3.7	1.2	3.3	1.2
	T_d			
All	8.1	4.0	10.3	4.3
1	10.2	3.4	11.0	3.9
2	7.5	3.9	10.5	4.6
3	8.4	3.8	9.0	4.1
	CM5 SP 2		CM7 SP 2	
	Average	Std.Dev	Average	Std.Dev.
	$k_v \times 10^2$			
All	2.2	0.8	4.7	2.4
1	2.1	0.6	5.1	2.6
2	2.3	0.8		
3	2.1	0.7	4.4	2.1
	T_d			
	Average	Std.Dev	Average	Std.Dev.
All	12	4.6	9.2	3.9
1	13.7	5.0	8.9	3.7
2	10.1	4.8		
3	13.7	4.2	9.7	3.7

The T_d results are also demonstrated in the Figure 18 where the average delay time per cement type for each CM and SP is also computed and compared. The gain k_v is higher in the case of the CEM II B-M (P-L) cement in comparison with the two other types, which means that for an input u an elevated output e is derived. CEM IV presents in any case the lower gain, because the most portion of the fly ash does not pass from the mill as it is fed directly to the dynamic separator. For this also reason the delay time of the CEM IV is the lower among the three cement types. The CEM A-L because of the elevated clinker content presents the higher delay time as it is the cement of the lower grindability. The standard deviations of the gains for each cement type do not differ noticeably from the total one. On the other hand the T_d standard deviations are in general lower for each cement type than the overall one.

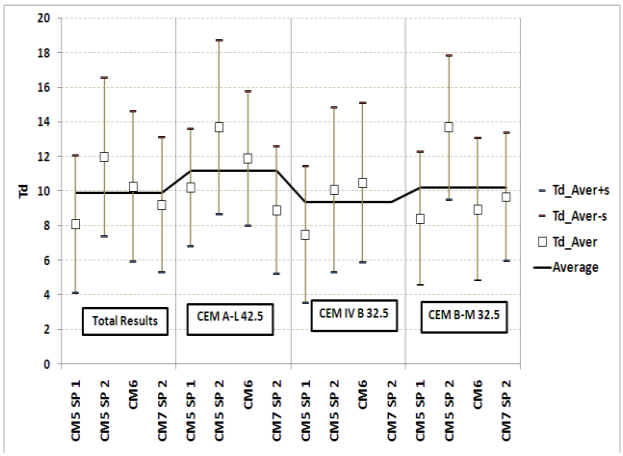

Figure 18. T_d for different cement types

The transfer function plots for the different mills and the main cement types ground to each one are depicted in the Figure 19. The significant difference of the transfer functions for the various cement types in the same CM is obvious from this figure.

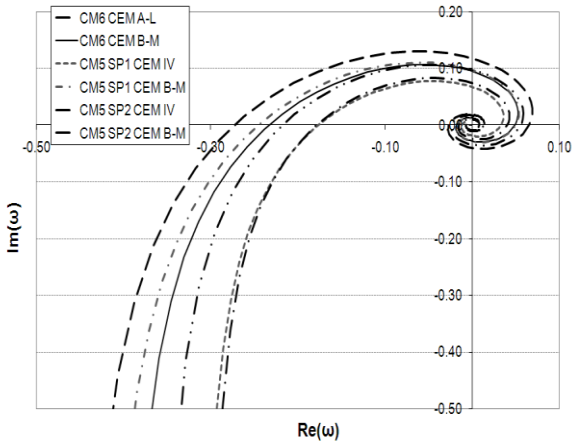

Figure 19. Niquist plots of the different cement types transfer functions

As a conclusion the grinding of different cement types to the same mill, has a severe impact on the model uncertainty, as in general the parameters for

each type differ significantly. The above generates problems in the tuning of a controller: If the controller is adjusted according to the average parameters, then this selection is not generally optimal for each cement type. If the tuning is based on the dynamic of one cement type, probably the regulation is not good for the other types. Apparently a fine solution is to dedicate as much as possible each cement mill for one cement type.

3.5 Impact of the Ball Charge Condition on the Parameters Uncertainty

It well known that the grinding media charge as total load and as composition as well, has a very strong effect on the CM productivity and product quality. A good indication of the current ball volume is the CM absorbed power, as the two variables are linearly related: For each specific mill, the process engineers have knowledge how many KW absorbs one ton of balls and they use this value to add balls in the CM, when the absorbed power drops.

To investigate the impact of the ball charge on the model parameters the following procedure is designed and performed:

- For each CM and cement type the set of data including the dynamic parameters is sorted according to the absorbed power.
- The data are separated in two subsets of higher and lower power. For the case of CM5 SP 2 the power difference between the two sets was not significant, less than 30 KW. So these data were excluded from further processing
- The average values of model parameters and power are calculated for each subset. Five cases are processed in total.

The results are presented in the Table 11.

Table 11. Impact of the CM power on the model parameters

T_d	$k_v \times 10^2$	Cem. Type	Mill KW
CM6			
11.6	3.2	1	1824
12.3	2.9	1	1901
8.4	3.6	3	1817
9.5	3.1	3	1889
CM5 SP 1			
7.0	3.1	2	799
7.7	2.9	2	854
9.4	3.2	3	815
7.9	4.2	3	874
CM7			
8.9	5.1	1	951
10.2	4.4	1	1157

In four out of the five cases studied, as the CM power increases, the gain drops and the delay time increases. Consequently the condition of the ball charge is a strong factor affecting the total model uncertainty. The physical meaning of these results is the following: As the ball charge is new and high, the mill productivity is higher, for given quality targets. So an increase of the variable $Q\text{-}Q_0$, causes less return, because the CM grinds finer resulting in lower $KW\text{-}KW_0$, comparing with the low power case. For this reason the gain is lower in the case of the high mill power. For fresh grinding media charge and high power, because of the better grinding, the increase of the feed Q, causes a slower increase of the return flow rate in comparison with the low power condition. Therefore the increase of the elevator power is delayed resulting in an increase of the model delay time.

4 Applied Techniques of PID Tuning

It is critical in control system design and tuning to assure the stability and performance of the closed loop in the case that a mismatch between accepted and actual model occurs, i.e. to guarantee robustness.

The feedback loop of the system to be controlled is given in the simplest possible form in the Figure 20.

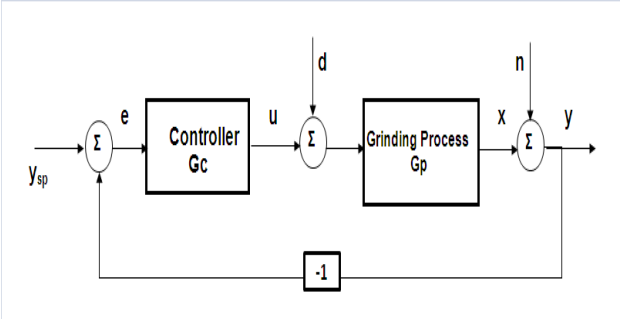

Figure 20. Feedback control loop

The system loop is composed from the grinding process G_p and the controller G_c. The grinding process is influenced by the controller via the variable u that is the mill feed. With the fresh feed also enter in the mill its characteristics as composition, grindability, temperature. The above represent a part of the disturbance d. Another portion of the disturbance represents the gas flow rate and its temperature. A third also portion can represent the mass flow of the separator return and the corresponding physical and chemical characteristics. For example a step change to the separator speed or to the gases passed from the separator, causes a change to the return flow rate

and its characteristics and consequently a further disturbance to the grinding operation. Apparently such adjustments sometimes are desirable for quality purposes, depending of the final product measured characteristics. These short term disturbances affect the process model accuracy and they have a certain impact on the model regression coefficient. As process output x, the recycle elevator power is considered that shall be controlled. Control is based on the measured signal y, where the measurements are corrupted by measurement noise n. Information about the process variable x is thus distorted by the measurement noise. To smooth the variable x, a first order filter with time constant T_f is added in the three CM under consideration by paying a relatively delayed response of the system. This time constant is selected notably less that the system delay time after some first evaluations of this variable and by experience as well. The controller is a system with two inputs: The measured elevator power y and the elevator set point y_{st}. The difference $y_{st} - y$ provides the signal error e. The controller transfer functions G_c is given by the typical form (14) according to Angstrom and Hagglund [10]. The variables k_p, k_i, k_d represent the proportional, integral and differential coefficients of the controller correspondingly.

$$\frac{u}{e} = k_p + \frac{k_i}{s} + k_d s \tag{14}$$

The same equation expressed in time difference form, to be possible to be passed in the CM operating system, is expressed by the equations (15), (16) where Δt is the sampling period in seconds:

$$e_n = y_{st} - y \tag{15}$$

$$u_n = u_{n-1} + k_p \cdot (e_n - e_{n-1}) + \frac{\Delta t}{60} \cdot k_i \cdot e_n + k_d \cdot \frac{1}{\Delta t} \cdot (e_n + e_{n-2} - 2 \cdot e_{n-1}) \tag{16}$$

Probably the best criterion of performance is the sensitivity function determined by the Laplace equation (17):

$$S = \frac{1}{1+G_c G_p} \tag{17}$$

An additional function to characterize the performance is also the complementary sensitivity function provided by the equation (18):

$$T = \frac{G_c G_p}{1+G_c G_p} \tag{18}$$

Apparently S+T=1. The function S tells how the closed loop properties are influenced by small variations in the process [14]. The maximum sensitivities represented by the equation (19) can be used as robustness measures.

$$M_s = Max\big(S(i\omega)\big) \qquad M_t = Max\big(T(i\omega)\big) \tag{19}$$

The variable $1/M_s$ can be interpreted as the shortest distance between the open loop G_cG_p Nyquist curve and the critical point (-1,0) shown in the Figure 21. In the same figure other also system properties, characterizing the system stability are shown:

- the gain margin, g_m
- the gain crossover frequency, ω_{gc}
- the phase margin, φ_m
- the sensitivity crossover frequency, ω_{sc}
- the maximum sensitivity crossover frequency, ω_{mc}.

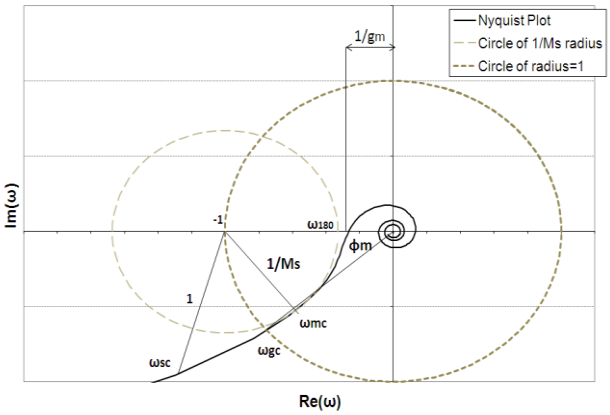

Figure 21. Maximum sensitivity, phase margin and crossover frequencies

Aiming to regulate the grinding system, subjected in multiple disturbances, with the purpose to achieve a good product quality with a high productivity, two widely used techniques are applied:

- The Internal Model Control – IMC – as described by Rivera [21] and Arbogast and Cooper [43] for integrating processes as under the selected operating conditions the process contains integration.
- The M-constrained integral gain optimization – MIGO – developed by Astrom, Panagopoulos and Hagglund [32, 34], belonging to the loop shaping methodology.

The performance of the implemented controllers is assessed in the following way:

- By building the convenient software, the daily CM data are loaded.
- The period of sampling is one minute. Therefore in 24 hours, up to 1440 points are loaded. The time period that the CM is stopped is excluded easily by the software, taking into account the mill motor power.
- Using the software, an effort is made to detect automatically the period that the CM runs in automatic mode, as when the CM starts to operate and up to be the circuit loaded, the manual mode is necessary.
- For a given set point of the power, KW_{sp}, the automatic mode operation performance is evaluated via the Integral of Absolute Error – IAE – computed by the Equation (20).

$$IAE = \frac{1}{t_0}\int_0^{t0} \left| KW(t) - KW_{sp} \right| dt \qquad (20)$$

4.1 Implementation of the IMC technique

The IMC tuning is applied to regulate the recycle elevator in two out of the three CM: CM5 and CM7. Before this technique to be selected, the PID parameters were adjusted by trial and error and the operation was in general satisfactory. The three controller parameters are calculated using the system of equations (21):

$$T_C = \alpha \cdot T_d \sqrt{10} \qquad k_P = \frac{1}{k_v} \cdot \frac{2 \cdot T_C + T_d}{\left(T_C + 0.5 \cdot Td\right)^2}$$

$$T_{Int} = 2 \cdot T_C + T_d \qquad T_{Deriv} = \frac{0.25 \cdot {T_d}^2 + T_C \cdot T_d}{2 \cdot T_C + T_d} \qquad (21)$$

$$k_i = \frac{k_p}{T_{Int}} \qquad k_d = k_p \cdot T_{Deriv}$$

Where T_c is a time parameter (min) connected with the time constant of the feedback control loop and consists a design parameter, determined by the value of the tuning parameter α. A value of α=1corresponds to typical design, while a value equal to 5 to conservative one. As concerns the maximum sensitivity M_s, a predetermined constraint is not put implicitly, but it is computed after the calculation of the open loop transfer function, at it depends on the value of the α parameter. For the calculation of the design parameter T_c a value α=1 has been considered for CM5, while α=0.7 for CM7, to provide a similar T_c value 31 to 32 min. The PID tuning was made after a sufficient number of data was collected for a period of at least 20 days. Then the PID with the tuned coefficients was put in operation. The results are depicted in the Table 12. For comparison reasons the PID parameters derived with trial and error are shown in the Table 13. Based also on the experience, minimum and maximum permissible feed flow rates are added to the controllers.

Table 12. PID parameters after IMC application

	Elevator ascent	Elevator descent	Elevator ascent	Elevator descent
	CM5		CM7	
k_p	1.43	2.15	1.31	1.43
k_i	0.03	0.03	0.019	0.021
k_d	5.2	7.0	7.7	8.4

Table 13. PID parameters found with trial and error

	Elevator ascent	Elevator descent	Elevator ascent	Elevator descent
	CM5		CM7	
k_p	0.6	0.6	0.6	0.6
k_i	0.03	0.04	0.03	0.04
k_d	7.0	8.0	7.0	8.0

The performance comparison between the two sets of PID parameters for each CM is executed using the daily IAE.

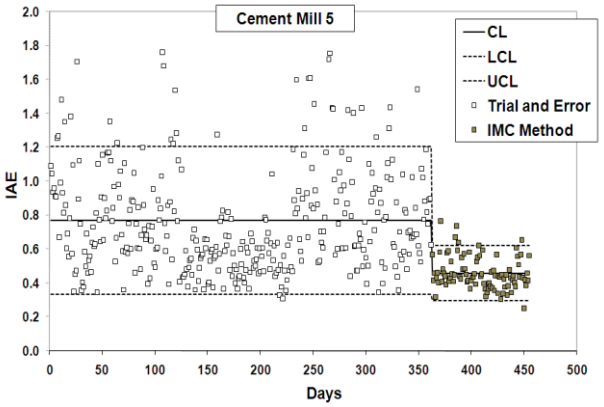

Figure 22. IAE comparison for CM5.

Furthermore, using the equations (10)-(12) the outlying IAE are detected and excluded and a control chart for each CM is constructed according to ISO 8258:1991. Subsequently the average IAE and the portion of outliers comparing to the total population for each parameters set is found. The above result in a further comparison between the two parameter sets for each mill. The daily IAE are illustrated in the Figures 22 and 23 for CM5 and CM7 respectively. In the same figures the average IAE and the upper and low 3σ limits after the

outliers' rejection are also demonstrated. The evaluation of the controllers' robustness using the two parameters sets is shown in the Table 14.

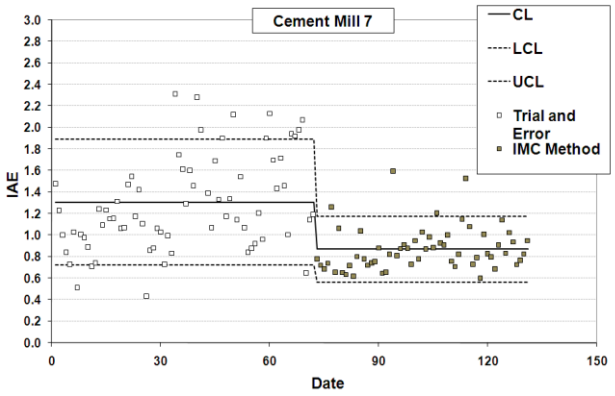

Figure 23. IAE comparison for CM7

Table 14. Performance comparison

	CM5	CM7
SP (KW)	18	28
IAE_{Aver} Trial and Error (1)	0.769	1.308
% IAE_{Aver}/SP	4.27	4.67
IAE_{Aver} IMC (2)	0.459	0.871
% IAE_{Aver}/SP	2.55	3.11
% (2) / (1)	59.7	66.6
IAE_{MAX} Trial and Error (3)	1.206	1.893
IAE_{MAX} IMC (4)	0.622	1.177
% (4) / (3)	51.5	62.2
% Outliers - Trial and Error (5)	9.9	16.7
% Outliers - IMC(6)	5.4	6.8
% (6) / (5)	54.0	40.7

Table 15. Maximum sensitivity gain and phase margin

	CM5		CM7	
	Ascend.	Desc.	Ascend.	Desc.
	Trial and Error			
M_S	2.9	3.4	2.9	5.8
g_m	5.0	4.4	3.1	2.9
φ_m	20.0	18.5	19.8	16.2
	Internal Model Control			
M_S	1.4	1.6	2.0	2.2
g_m	5.7	4.1	2.0	1.9
φ_m	46.0	52.5	45.4	45.2

The maximum sensitivities M_s and the gain and phase margins g_m and φ_m for each group of parameters are shown in the Table 15. The average model parameters, shown in the Table 4 are used to determine the above variables. Because different dynamic model is applied when the elevator power ascends or descends, different open loop properties are also computed. The superior performance of the controllers tuned using IMC against them tuned with trial and error becomes more than obvious from the figures 22, 23 and the Table 14. The explanation of this enormous difference is provided by the results of the Table 15. The M_S in the IMC case is significantly less than this of the trial and error case. In spite that M_S is not contained as constraint in the IMC tuning, by experience the T_C design parameter was chosen so that to be inside the grinding system response time. In this way M_S is found in the area of 1.4 to 2.2 for the four parameter sets. In the tuning with trial and error more attention was given to be the system stable, as without a design tool it is around impossible to proceed further and to try to optimize the performance under the high uncertainty conditions characterizing the grinding process.

Further detailed investigation related with the effect of the model uncertainty on the short term sensitivities and gain and phase margins will be presented in the analysis of the obtained results by tuning the controllers with the MIGO method.

4.2 Implementation of the MIGO technique

4.2.1 Short Description and Tuning Procedure

The M-constrained integral gain optimization method is presented and analyzed thoroughly in [32], [34]. In this case the dynamic model average parameters are derived from a bigger set of initial experimental data than in the IMC case.

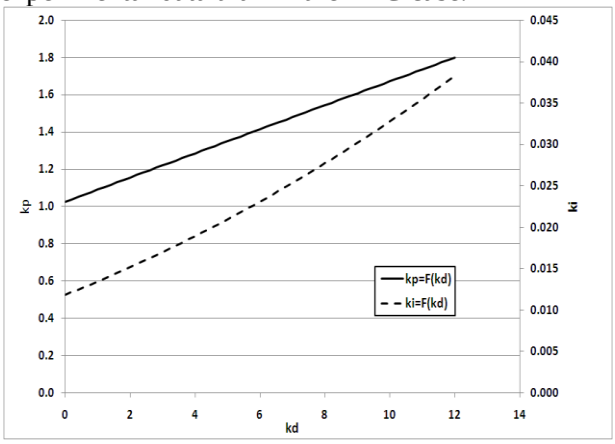

Figure 24. Function between the controller parameters.

A constraint in the M_S is placed and the sets (k_p, k_i, k_d) are computed, starting from k_d=0 up to a

maximum value of k_d satisfying the M_s constraint. When k_d is maximum, the same occurs also for k_p, k_i. An example of the function between the three PID coefficients as k_d varies from 0 to a maximum value is provided in the Figure 24. The open loop transfer function is restricted to have $M_s \leq 1.5$. The dynamic parameters of CM5 for SP 2 are considered. From this figure it is concluded that a change of k_d from 0 to 12 causes an 80% increase of k_p while the k_i is augmented by three times. In parallel the constraint of M_s is always fulfilled. The open loop Nyquist functions for kd=0, 3, 7, 10 are shown in the Figure 25.

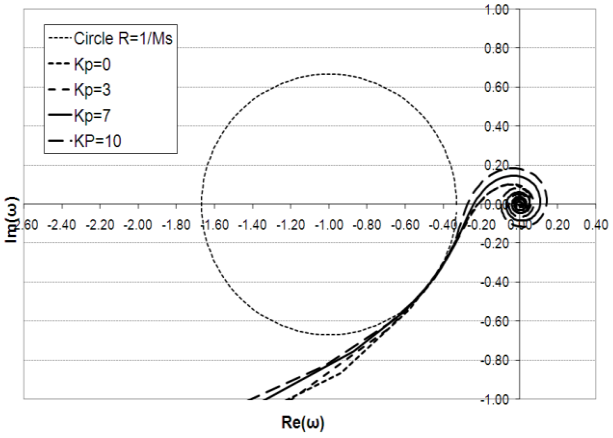

Figure 25. Niquist plots for M_s=1.5 and different k_p

Consequently the applied loop shaping technique possesses the great benefit to provide for the same maximum sensitivity a set of parameters satisfying this constraint. From this set a corresponding set of gain and phase margins can be determined. By varying k_d from 0 to 11, the range of these margins are obtained and illustrated in the Figure 26.

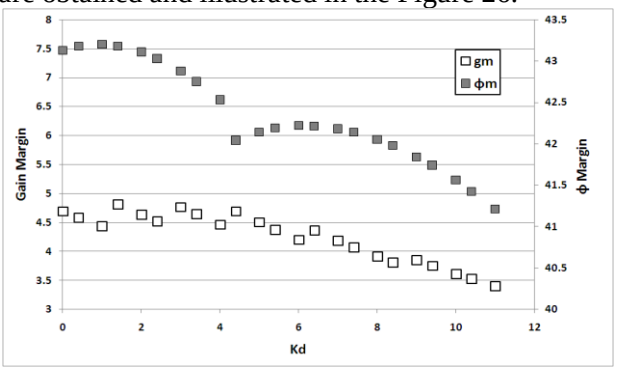

Figure 26. Gain and phase margins as function of k_d

As the differential part increases, both gain and phase margins are decreasing. Therefore the k_d and the corresponding coefficients set shall be selected with one of the following ways:

(a) To take a k_d near to the middle of the range.
(b) To decide according to a designed or predetermined gain or phase margin.
(c) To determine the k_d providing the minimum IAE using some kind of simulation of the real operation.

4.2.2 Controllers Parameterization and IAE results

In the level of development of this research, the set of parameters is selected using a k_d in the middle of the acceptable range for a predetermined M_s. The parameter values for the different CM and recycle elevator set points are provided in the Table 16.

Table 16. PID coefficients tuned with MIGO

	CM5 SP 1	CM5 SP 2	CM7 SP 1	CM7 SP 2
k_p	1.61	1.90	1.07	1.07
k_i	0.043	0.027	0.025	0.025
k_d	7.0	7.0	7.0	7.0
	CM6			
k_p	1.3			
k_i	0.03			
k_d	7.0			

As in the case of IMC, the tuning with MIGO was based on the existing dynamic data when this procedure was performed and not on the full data set deriving the parameters of the Tables 5 and 6. The daily IAE for the three CM and the different set points are depicted in the Figures 27, 28, 29.

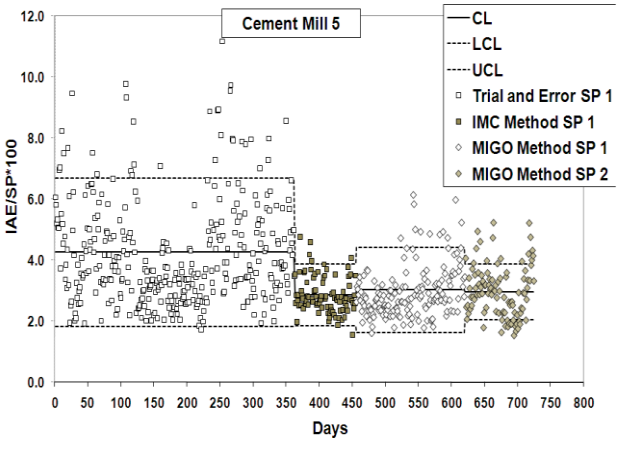

Figure 27. %CV of IAE for CM5

To compare better for the various set points, but also between cement mills results, the IAE are expressed as %CV of IAE, by the formula $\frac{IAE}{SP} \cdot 100$. In the same figures the %CV of IAE by applying trial and error and IMC tuning are also shown. As

regards the IAE of CM5 is the same for both methods: IMC and MIGO. In the case of CM6, the IAE when MIGO is utilized is largely better than the previous trial and error tuning. Using MIGO tuning the IAE in the case of CM7 is significantly less than the one obtained by applying IMC tuning. For CM5, CM7 the reasons will be investigated by studying the properties of the open loop transfer functions. The average IAE, the maximum sensitivities and the gain and phase margins for each case examined are shown in the Table 17.

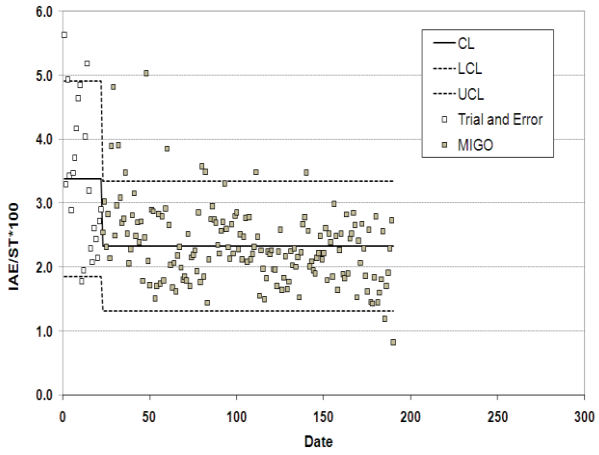

Figure 28. %CV of IAE for CM6.

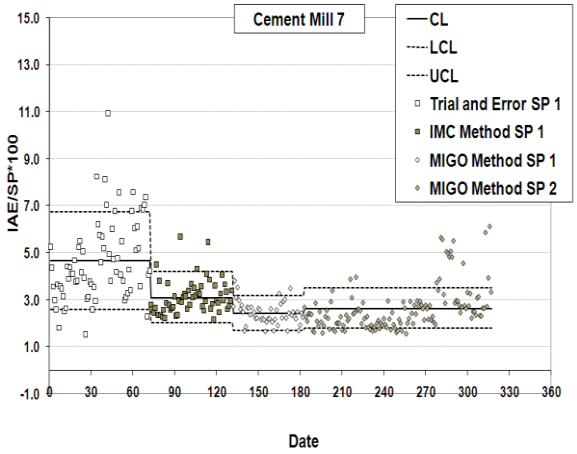

Figure 29. %CV of IAE for CM6.

Table 17. Controllers performance tuned using MIGO

	CM5	CM5	CM6	CM7	CM7
SP	18	26.7	36.6	28	30
IAE	0.24	0.24	0.43	0.34	0.40
% IAE/SP	3.03	2.97	2.34	2.44	2.66
M_S	1.50	1.65	1.48	1.50	1.50
g_m	3.98	3.18	3.78	3.09	3.09
φ_m	41.9	41.4	41.9	47.5	47.5

While the parameterization of CM5 for SP=26.7 was performed for M_S = 1.5, due to the model parameters uncertainty, the used parameters had a small difference from the ones shown in the Table 6 resulting in a higher M_S. The improvement of IAE of CM7 using MIGO compared with the IAE by utilizing IMC is caused to the lower M_S of the controller compared with the former case. Using the MIGO method to adjust the PID parameters the IAE achieved is 2.3-3% of the set point in spite the model parameters uncertainty.

4.2.3 Impact of the model uncertainty on the open loop properties

The model parameters shown in the Tables 5 and 6 are determined as the average of the values calculated for each set of input and process variables. The uncertainty of these variables is also expressed by the coefficient of variation of the natural deviation σ_{Nat}. To study the influence of model parameter uncertainty in the daily achieved sensitivity, phase and gain margins of the open loop function $G_c \cdot G_p$ the following procedure is applied:

(a) For each CM and set point the applied PID parameters are considered.
(b) For each set of experimental data the open loop properties are computed.
(c) The average and standard deviation of each property is found
(d) From the previous step the %CV of each open loop characteristic is determined.

The %CV of the model parameters as well as of the open loop characteristics are shown in the Table 18. It becomes obvious from this table that the model uncertainty not only is not attenuated but in some cases is amplified.

Table 18. %CV of model parameters and of open loop characteristics

CM	SP	k_v	T_d	M_S	g_m	φ_m
CM5	18.0	27.6	41.6	29.7	86.5	29.8
CM5	26.7	28.7	34.1	31.7	93.0	29.3
CM6	36.6	35.7	39.0	31.9	52.2	26.9
CM7	28.0	36.1	34.4	39.2	52.7	27.3
CM7	30.0	33.4	38.2	27.8	63.4	28.1

In spite the fact of the big variance of the daily open loop properties, the controllers adjusted with the MIGO technique behave with great robustness as the %CV of IAE is found in the range of 2.3-3%. Although the controllers are tuned for M_S=1.5 using a subset of the total experimental data, the big

variance of the daily M_s derives an average M_s usually a few higher from the designed one. An example of maximum sensitivity distribution for the results of CM5 and both set points is presented in the Figure 30.

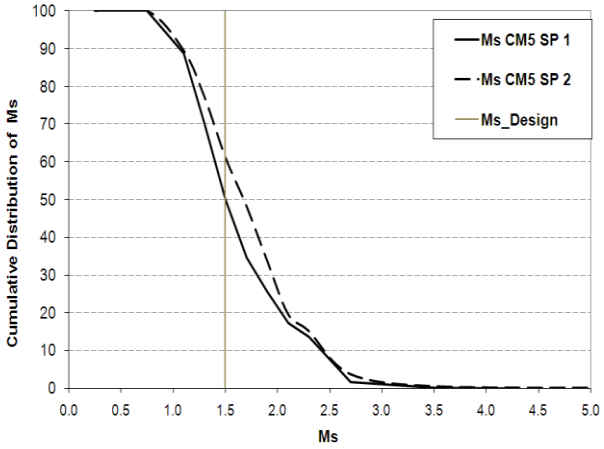

Figure 30. M_s cumulative distribution for CM5

As it is mentioned earlier MIGO provides a full group of (k_p, k_i, k_d) parameters ranging from k_d=0 to a maximum value fulfilling the constraint of M_S as to the open loop transfer function. If no other constraint is set, then k_d is the design parameter. Based on actual data sets and for a predefined M_S, an investigation is carried out concerning the impact of the k_d value on the data set average M_S and its standard deviation.

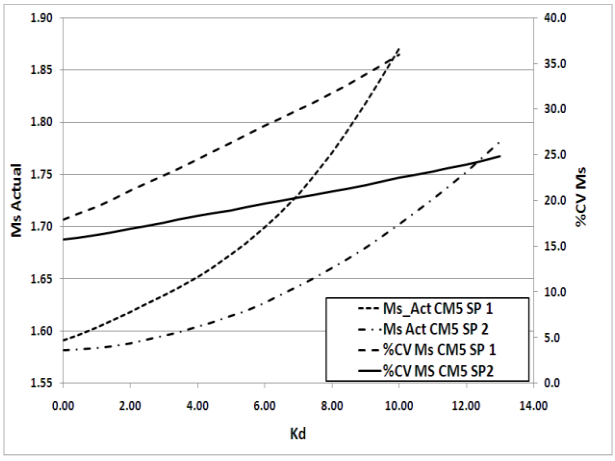

Figure 31. Average and standard deviation of M_s as function of k_d.

The dynamic parameters of CM5 SP1 and CM5 SP2 are considered. Using them the PID coefficients are computed for M_s = 1.5 and an array of (k_p, k_i, k_d) is obtained. Then for the dynamic parameters of each data set the individual M_s are found and their average and standard deviation as well. The results are depicted in the Figure 31.

As k_d increases, the average M_s and its standard deviation grow too. After a certain k_d value, average M_s deviates notably from the designed one. To avoid this undesirable phenomenon, probably it is better to design with a lower M_s, to be able to tune the parameters with a higher k_d.

To examine the effect of the predetermined M_s according to the design on the population average M_s and its variance, the following procedure is executed:

(a) The CM5 SP 2 data sets are considered and the individual dynamic of its set.
(b) Two values of k_d are chosen: k_d = 2 and k_d =8.
(c) The M_s constraint is getting values in the interval [1.5, 2.0] for SP 1 and [1.3, 2.3] for SP2
(d) The population average and a maximum $M_{s,\,80}$ are computed. In the interval [0, $M_{s,\,80}$] the 80% of the Ms population is contained.

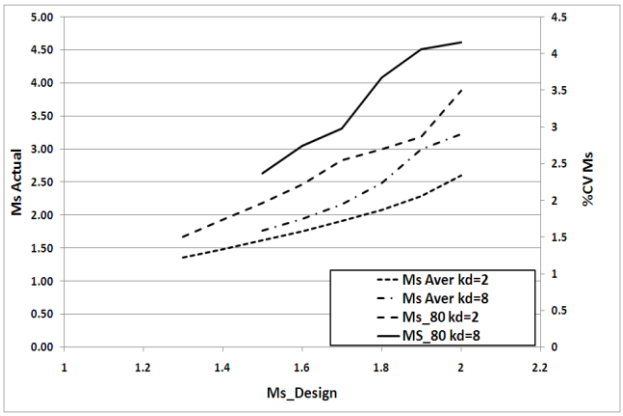

Figure 32. Average and standard deviation of M_s as function of the M_s constraint for CM5 SP 1.

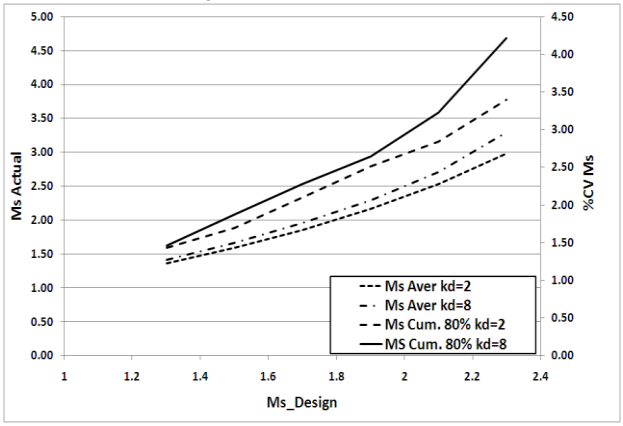

Figure 33. Average and standard deviation of M_s as function of the M_s constraint for CM5 SP 2.

The results are shown in the Figures 32 and 33 for SP 1 and SP 2 respectively. Similar to these figures

are also obtained for the two other CM. From these figures the following conclusions can be extracted:

- For any designed M_S constraint the average of the actual population is higher than the designed.
- The difference between actual average and designed M_S is amplified as the designed constraint increases.
- As the constrain increases the critical M_{S80} also is considerably growing.
- For the grinding closed circuits under investigation, a robust design shall have as maximum M_S limitation a value of 1.6, in order to permit a maximum actual average M_S of 2.0.

4.2.4 MIGO design for different cement types

As it is in detail described in section 3.4, different cement types ground in the same CM and for the same elevator set point, present diverse dynamic behavior resulting in different dynamic parameters depicted in the Table 10. Consequently this is one of the causes of the model parameters uncertainty if the various cement types are not taken into account. To evaluate the effect of those dynamics on the open loop transfer function the subsequent procedure is built.

(a) For the average model parameters shown in the Tables 5, 6 the PID parameters are adjusted for an M_s=1.5 and k_d=7.
(b) For these dynamic parameters and PID coefficients, the open loop transfer function is found.
(c) For the same PID coefficients and the parameters shown in the Table 10, the open loop transfer function is determined for the main cement types ground to each CM.
(d) The resulting transfer functions are compared.

The derived parameters and the open loop properties are presented in the Table 19. It is easily concluded from this table that the open loop of cements containing more clinker – according to the Table 8 – and becoming harder to be ground, present elevated Ms, and lower g_m and φ_m. Therefore by applying PID controllers tuned using the average model parameters, the easiness to regulate depends on the clinker content for the given cement types.

The transfer functions obtained for CM6 are illustrated in the Figure 34 and it becomes clearer that the open loop transfer functions and consequently the typical controller performance differs for the various cement types. Subsequently, it should be examined if there are PID coefficients applied to the average dynamic of each cement type deriving controllers of the same performance as the one obtained with the average model parameters.

Table 19. PID coefficients and open loop characteristics for average model

	CM5 SP 1	CM5 SP 2	CM6
k_p	1.626	1.477	1.329
k_i	0.042	0.0254	0.0304
k_d	7.0	7.0	7.0
	Average Dynamics		
M_S	1.50	1.50	1.50
g_m	3.95	4.18	3.74
φ_m	41.9	42.1	41.8
CEM Type	2	2	1
M_S	1.40	1.38	1.70
g_m	4.50	4.57	3.26
φ_m	45.4	46.7	36.1
CEM Type	3	3	3
M_S	1.57	1.65	1.42
g_m	3.25	3.72	3.84
φ_m	41.7	37.6	44.7

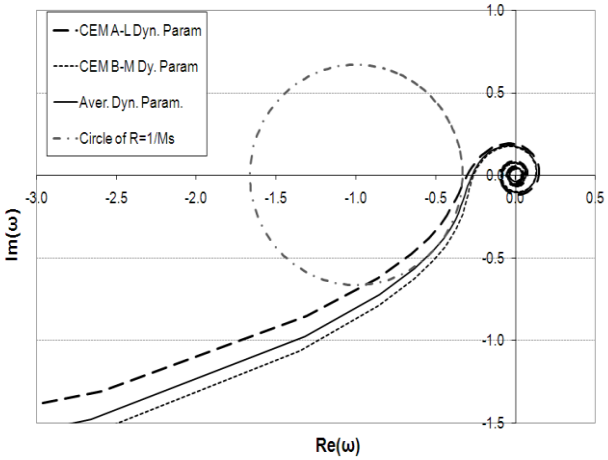

Figure 34. Nyquist plots for CM6 and different cement types.

To investigate the above, MIGO is applied using the model of each cement type for each CM. If for a cement type and according to Table 19 M_s > 1.5, then the constraints M_s=1.5 and k_d=7 are considered. Otherwise if according to Table 19 M_s<1.5, this value has been taken as constraint. The k_d value is chosen to provide the same gain margin as the one depicted in the former Table for the mentioned cement type. The results are presented in the Table 20.

Table 20. PID coefficients and open loop characteristics for each cement type model

	CM5 SP 1	CM5 SP 2	CM6
k_p	1.626	1.477	1.329
k_i	0.042	0.0254	0.0304
k_d	7.0	7.0	7.0
	Average Dynamics		
M_S	1.50	1.50	1.50
g_m	3.95	4.18	3.74
φ_m	41.9	42.1	41.8
CEM Type	2	2	1
k_p	1.664	1.479	1.18
k_i	0.0434	0.0269	0.023
k_d	7.0	7.0	7.0
M_S	1.40	1.4	1.50
g_m	4.45	4.58	3.65
φ_m	45.4	45.4	41.6
CEM Type	3	3	3
k_p	1.445	1.31	1.287
k_i	0.0418	0.0198	0.0296
k_d	7.0	7.0	7.0
M_S	1.50	1.50	1.40
g_m	3.59	4.05	3.90
φ_m	41.5	41.8	45.0

The PID controllers with parameters shown in this Table are applied for each CM and cement type to the individual data sets and dynamics. The M_S of each data set is computed and for each type of cement, the respective average and standard deviation of the M_S are determined. The results are demonstrated in the Table 21.

Table 21. Comparison of M_S statistics

	Aver. Ms	Std. Dev. Ms
Cement Type	CM6 CEM CODE: 1	
Aver. Dyn.	1.87	0.64
CEM Type Dyn.	1.63	0.35
	CM6 CEM CODE: 3	
Aver. Dyn.	1.63	0.67
CEM Type Dyn.	1.58	0.41
	CM5 SP 1 CEM CODE: 3	
Aver. Dyn.	1.86	0.56
CEM Type Dyn.	1.73	0.50
	CM5 SP 1 CEM CODE: 2	
Aver. Dyn.	1.62	0.45
CEM Type Dyn.	1.61	0.45
	CM5 SP 2 CEM CODE: 3	
Aver. Dyn.	1.47	0.27
CEM Type Dyn.	1.49	0.29
	CM5 SP 2 CEM CODE: 2	
Aver. Dyn.	1.75	0.34
CEM Type Dyn.	1.56	0.24

It can be clearly observed that when the PID of each CM is tuned according to the cement type ground, the average and standard deviation of M_s is lower than the statistics determined by an average model for all the cements ground to this mill. This is a very important conclusion as to the PID tuning: In a given cement plant, it is not enough to adjust the controller parameters in each cement mill, but the cement types processed shall be taken into consideration. The mill PID parameterization per cement type results in more robust controllers of reduced divergence between actual and designed M_s. The above can be considered as a consequence of the rejection of a continuous source of uncertainty.

4.2.5 Effect of the mill power on the PID tuning

From Table 11 it is derived that as the CM power increases, the gain drops and the delay time increases. The reasons are explained in detail in the section 3.5. Subsequently for each power interval and predetermined M_s constraint, a different set of PID parameters is necessary for the same CM and the same cement type. For the dynamic parameters shown in Table 11 and the M_S constraints presented in Table 20 the PID coefficients are derived for each CM, cement type and power interval. The results are shown in Tables 22, 23.

Table 22. PID tuning as function of CM power – CM5, CM6

	CM5	CM5	CM5	CM5
SP	18	18	18	18
Type	2	2	3	3
Power	799	854	815	874
k_p	1.649	1.53	1.432	1.353
k_i	0.0443	0.0359	0.0357	0.0414
k_d	7.0	7.0	7.0	7.0
M_S	1.40	1.40	1.50	1.50
g_m	4.34	4.28	3.70	3.31
φ_m	45.3	45.0	41.4	41.0
	CM6	CM6	CM6	CM6
SP	36.6	36.6	36.6	36.6
Type	1	1	3	3
Power	1824	1901	1817	1889
k_p	1.146	1.224	1.36	1.235
k_i	0.0228	0.0233	0.0351	0.0254
k_d	7.0	7.0	7.0	7.0
M_S	1.50	1.50	1.40	1.40
g_m	3.54	3.78	3.83	3.96
φ_m	41.5	41.8	44.0	44.2

Table 22. PID tuning as function of CM power – CM7

	CM7	CM7
SP	28	30
Type	1	1
Power	951	1157
k_p	1.032	1.035
k_i	0.0297	0.0255
k_d	6.0	6.0
M_S	1.50	1.50
g_m	3.11	3.35
φ_m	41.4	41.3

The efficiency of the MIGO technique is also proven in this case, as for dynamics corresponding to different average absorbed power in the CM motor, MIGO is able to design PID's of similar characteristics and performance. According to these results and based on the paste experience as regards the power absorption in every CM, each period between two consecutive addition of new ball charge can be divided in two sub-periods. The model parameters and the PID coefficient of each time interval can be adjusted according to the historical data. Therefore by attenuating the effect of an additional permanent source of model uncertainty, the PID tuning and the controller performance are enhanced.

6 Conclusions

In the present study the dynamic behavior of three closed circuit cement mills is investigated by utilizing industrial scale data received online. In this way the laborious experimentation, creating problems to the mill operation and to the product quality is avoided. The technique applied can be characterized as "plant friendly" system identification [44].

The model fitting the data involves integration. Using non linear regression techniques the model parameters are determined as well as their uncertainty. It is confirmed that the selected models describe adequately the process, as the 75-85% of an amount of more than 2600 experimental data sets, presents a regression coefficient more than 0.7. For the period under consideration, the gain uncertainty varies from 28% to 36%, while the delay time uncertainty is found between 34% and 42%.

The grinding of different cement types to the same mill is identified as one of the major reasons of the model uncertainty. The above obviously could cause difficulties to the robust tuning of a controller. Consequently, as more dedicated is each cement mill to grind one cement type, more regular is its operation and the controller tuning becomes more efficient. The level and condition of grinding media and consequently the mill motor power is another relatively strong factor of model uncertainty.

Two tuning techniques are applied to adjust the PID coefficients: The Internal Model Control (IMC) and the M - Constrained Integral Gain Optimization (MIGO). To implement IMC, a simplified dynamic model is considered, without to take into account the first order filter utilized to smooth the process variable. While in MIGO the filter time constant is incorporated in the model.

In spite the simplicity of the IMC version applied, a good enough regulation of two CM is achieved, much better than the previous one, based on trial and error parameters tuning. The comparison is based on the daily IAE. In MIGO technique, M_s constitutes a primarily considered by the method constraint, to guaranty the controller robustness. For the same M_s a set of PID coefficients are provided, starting from a typical PI controller up to a maximum k_d value, fulfilling the maximum sensitivity constraint. The implementation of the MIGO technique derives robust controllers, with performance superior of IMC or at least equal as to IAE. For all the cases studied the daily average IAE is from 2.3% to 3% of the set point value. The selection of the optimum (k_p, k_i, k_d) set, needs further investigation using more precise simulations of each mill operation.

Two of the main causes of model uncertainty are mentioned: The grinding of several cement types in the same CM and the decrease of the mill absorbed power during the time. By determining the average model parameters for each case, then the CM controller can be tuned according to the cement type ground and the power absorbed. In an actual grinding circuit, the PID coefficients could be changed automatically, taking into account the former data – cement type and mill motor power. The above can result in severe improvement of the controller performance.

References:

[1] Clemens P., Effective automation of closed circuit bucket elevator mills for cement, *VDZ Congress, Process Technology of Cement Manufacturing,* Dusseldorf, 2002, pp. 116- 122

[2] Espig D. and Reinch V., Advantages of Computer Based Mill Audits, and Simulation using Selected Cement Grinding Plants, *VDZ Congress, Process Technology of Cement Manufacturing, Dusseldorf, 2002,* pp. 123- 134.

[3] Ramasamy, M., Narayanan, S.S, Rao, Ch.D.P., Control of ball mill grinding circuit using model

predictive control scheme, *Journal of Process Control*, 2005, pp. 273-283.

[4] Chen, X., Li, Q., Fei, S., Constrained model predictive control in ball mill grinding process, *Powder Technology*, Vol. 186, 2008, pp. 31-39.

[5] Efe, M.O., Kaynak, O., Multivariable Nonlinear Model Reference Control of Cement Mills, *15th Triennial World Congress*, Barcelona, 2002.

[6] Chai, T.Y., Yue, H., Multivariable Intelligent Decoupling Control System and its Application *Acta Automatica Sinica.*, Vol. 31, 2005, pp. 123-131

[7] Dagci, O.H., Efe, M.O., Kaynak, O., A Nonlinear Learning Control Approach For a Cement Milling Process, *Proceedings of the 2001 IEEE International Conference on Control Applications*, Mexico City, 2001, pp 498-503.

[8] Chen, X., Li, S., Zhai, J., Li, Q., Expert system based adaptive dynamic matrix control for ball mill grinding circuit, *Expert Systems with Applications: An International Journal*, Vol. 36, 2009, pp. 716-723.

[9] Qin, S.J., Badwell, T.H., A survey of industrial model predictive control technology, *Control Engineering Practice*, Vol. 11, 2003, pp. 733-764

[10] Astrom, K., Hagglund, T., Advanced PID Control, *Research Triangle Park: Instrumentation, Systems and Automatic Society*, 2006.

[11] Ender, D., Process Control Performance: Not as good as you think, *Control Engineering*, Vol. 40, 1993, pp.180-190

[12] Gao, Z., Scaling and bandwidth - parameterization based controller tuning, *Proceedings of the American Control Conference*, Vol. 6, 2003, pp. 4989-4996.

[13] Volosencu, C., Pseudo-Equivalence of Fuzzy PID Controllers, *WSEAS Transactions on Systems and Control*, Vol. 4, 2009, pp. 163-176.

[14] Astrom. K.J., Model Uncertainty and Robust Control, *Lecture Notes on Iterative Identification and Control Design*, Lund University, 2000, pp. 63–100.

[15] Astrom, K.J., Hagglund, T., The future of PID control, *Control Engineering Practice*, Vol. 9, 2001, pp. 1163–1175.

[16] Ziegler, J.G., Nichols, N.B., Optimum settings for automatic controllers, *Transactions ASME*, Vol. 64, 1942, pp. 759–768.

[17] Luyben, W. L., Simple method for tuning of SISO controllers in multivariable systems. *Industrial Engineering Chemistry Process Design Development*, Vol. 25, 1986, pp. 654-663.

[18] Garcia, C.E., Morari, M., Internal Model Control-1. A unifying review and some new results, *Ind. Eng. Chem. Process Des. & Dev.*, Vol. 21, 1982, pp.308-323.

[19] Garcia, C.E., Morari M., Internal Model Control-2. Design procedure for multivariable systems, *Ind. Eng. Chem. Process Des. & Dev*., Vol. 24, 1985, pp.472-484.

[20] Garcia, C.E., Morari, M., Internal Model Control-3. Multivariable control law computation and tuning guidelines, *Ind. Eng. Chem. Process Des. & Dev.*, Vol. 24, 1985, pp.484-494

[21] Rivera, D.E., Morari, M., Skogestad, S., Internal Model Control 4. PID Controller Design, Ind. Eng. Chem. Process Des. & Dev. Vol. 25, 1986, pp. 252-265

[22] Morari, M. Zafiriou, E., Robust Process Control, *Prentice Hall*, 1989.

[23] Yamada, K., Modified Internal Model Control for unstable systems, *Proceedings of the 7th Mediterranean Conference on Control and Automation (MED99)*, Haifa, Israel, 1999, pp. 293-302.

[24] Cooper, D. J., Practical process control. *Control Station*, Inc., 2004.

[25] Skogestad, S., Tuning for Smooth PID Control with Acceptable Disturbance Rejection, *Ind. Eng. Chem. Res.*, Vol. 45, 2006, pp. 7817-7822.

[26] Skogestad, S., Tuning for Smooth PID Control with Acceptable Disturbance Rejection, *Ind. Eng. Chem. Res.*, Vol. 45, 2006, pp. 7817-7822.

[27] McFarlane, D., Glover, K., A loop shaping design procedure using H_∞ synthesis, IEEE Transactions on Automatic Control, Vol. 37, 1992, pp. 759–769.

[28] Zolotas, A.C., Halikias, G.D., Optimal Design of PID Controllers Using the QFT Method, IEE Proc. – Control Theory Appl., Vol. 146, 1999, pp. 585-590

[29] Gorinevsky, D., Loop-shaping for Iterative Control of Batch Processes, *IEEE Control Systems Magazine*, Vol. 22, 2002, pp. 55—65.

[30] Yaniv, O., Nagurka, M. Automatic Loop Shaping of Structured Controllers Satisfying QFT Performance, *Transactions of the ASME*, Vol. 125, 2005, pp. 472-477.

[31] Hara, S., Iwasakiy,T., Shiokata, D., Robust PID Control via Generalized KYP Synthesis, *Mathematical Engineering Technical Reports*, 2005, pp. 1-18.

[32] Astrom, K.J., Panagopoulos, H., Hagglund, T., Design of PI controllers based on non-convex optimization, *Automatica*, Vol. 34, 1998, pp. 585–601.

[33] Hagglund, T., Astrom, K.J., Revisiting the Ziegler–Nichols tuning rules for PI control, Asian Journal of Control, Vol. 4, 2002, pp. 364–380.

[34] Panagopoulos, H. Astrom, K.J., Hagglund, T., Design of PID controllers based on constrained optimization, *IEE Proceedings-Control Theory and Applications*, Vol. 149, 2002, pp. 32–40.

[35] Astrom, K.J., Hagglund, T., Revisiting the Ziegler–Nichols step response method for PID control, *Journal of Process Control*, Vol. 14, 2004, pp. 635–650.

[36] Emami, T., Watkins, J.M., A Unified Approach for Sensitivity Design of PID Controllers in the Frequency Domain, *WSEAS Transactions on Systems and Control*, Vol. 4, 2009, pp. 221-231

[37] Emami, T., Watkins, J.M., Robust Performance Characterization of PID Controllers in the Frequency Domain, *WSEAS Transactions on Systems and Control*, Vol. 4, 2009, pp. 232-242

[38] Astrom, K., Hagglund, T., PID Controllers: Theory, Design and Tuning, *Research Triangle Park: 2nd Ed. Instrumentation, Systems and Automatic Society,* 1995.

[39] Rossiter J.A., Model Based Predictive Control, *CRC Press*, 2004.

[40] Austin, L.G. Crushing, Grinding and Classification, *Kluwer Academic Publishers*, 1996.

[41] Deniz V., The effect of mill speed on kinetic breakage parameters of clinker and limestone, Cement and Concrete Research, Vol. 34, 2004, pp.1365-1371.

[42] Morozov E.F., Shumailov V.K., Modified solution of the batch grinding equation, *Journal of Mining Science*, Vol. 19, 1992, pp. 43-47.

[43] Arbogast, J.E., Cooper, D.J., Extension of IMC tuning correlations for non-self regulating (integrating) processes, ISA Transactions, Vol. 46, 2007, pp. 303–311.

[44] Rivera, D.E., Lee, H., Braun, M.W., Mittelman, H.D., "Plant Friendly" System Identification: A Challenge for the Process Industries, *13th IFAC Symposium of System Identification,* Rotterdam, 2003